Rapid Communications

Proposal for the detection of magnetic monopoles in spin ice via nanoscale magnetometry

Franziska K. K. Kirschner,[1,*] Felix Flicker,[2,†] Amir Yacoby,[3] Norman Y. Yao,[2,4] and Stephen J. Blundell[1,‡]
[1]*Department of Physics, University of Oxford, Clarendon Laboratory, Parks Road, Oxford OX1 3PU, United Kingdom*
[2]*Department of Physics, University of California, Berkeley, California 94720, USA*
[3]*Department of Physics, Harvard University, Cambridge, Massachusetts 02138, USA*
[4]*Materials Science Division, Lawrence Berkeley National Laboratory, Berkeley, California 94720, USA*

(Received 24 October 2017; revised manuscript received 19 January 2018; published 17 April 2018)

We present a proposal for applying nanoscale magnetometry to the search for magnetic monopoles in the spin ice materials holmium and dysprosium titanate. Employing Monte Carlo simulations of the dipolar spin ice model, we find that when cooled to below 1.5 K these materials exhibit a sufficiently low monopole density to enable the direct observation of magnetic fields from individual monopoles. At these temperatures we demonstrate that noise spectroscopy can capture the intrinsic fluctuations associated with monopole dynamics, allowing one to isolate the qualitative effects associated with both the Coulomb interaction between monopoles and the topological constraints implied by Dirac strings. We describe in detail three different nanoscale magnetometry platforms (muon spin rotation, nitrogen-vacancy defects, and nanoscale arrays of superconducting quantum interference devices) that can be used to detect monopoles in these experiments and analyze the advantages of each.

DOI: 10.1103/PhysRevB.97.140402

Although fundamental magnetic monopoles have so far proven elusive, it has recently become possible to study properties of monopolelike excitations in condensed-matter systems [1]. The spin ices, in particular, dysprosium titanate [$Dy_2Ti_2O_7$ (DTO)] and holmium titanate [$Ho_2Ti_2O_7$ (HTO)] have been identified as promising candidates to host such elementary excitations [2–5]. The magnetic rare-earth-metal ions (Dy^{3+} or Ho^{3+}) and the nonmagnetic Ti^{4+} ions are arranged on two separate interpenetrating pyrochlore sublattices, each consisting of a network of corner-sharing tetrahedra. The rare-earth moments ($\approx 10\mu_B$) are well modeled as classical Ising spins, constrained by the crystal field to lie along the local $\langle 111\rangle$ axes. Exchange and dipolar interactions acting in this lattice geometry result in the four spins in each tetrahedron adopting a ground state in which two spins point towards and two away from the tetrahedron's center. This is termed the "ice rule," by analogy with protons in water ice [2,6]. This leads to a macroscopic degeneracy in the ground state with six possible spin configurations per tetrahedron.

The elementary excitations in spin ice consist of single flipped spins, which can fractionalize into a pair of monopoles, each traveling through the lattice by successive spin flips [3]. These monopoles manifest themselves as sinks and sources of magnetization, corresponding to tetrahedra in the three-in-one-out or one-in-three-out configurations [7–9]. Including the dipolar interactions between spins, the intermonopole interaction has the form of Coulomb's law, completing the analog to fundamental magnetic monopoles [3,10,11] and allowing the spin ice state to be described as a $U(1)$ classical spin liquid [12]. Unambiguous observation of the individual monopoles in spin ice would not only confirm this theoretical picture, but also allow these excitations and their dynamics to be studied directly. Previous attempts to identify the spin ice state share the common feature that they infer monopole behavior from the monopoles acting *en masse* [3,5,10,13]. The direct measurement of the microscopic magnetic field from individual monopoles remains an open challenge.

Recent developments have opened the door to new possibilities for the detection and characterization of magnetic textures on the nanometer scale. In this Rapid Communication, we employ Monte Carlo numerical modeling to provide both quantitative and qualitative predictions for what this next generation of nanoscale magnetometers will be able to probe when applied to spin ice at low temperatures. We conclude that measurements of the magnetic noise spectral density $S(\omega)$ will contain features arising from monopole dynamics due to both topological constraints arising from Dirac strings and long-range forces. We propose and analyze three different detection platforms: muon spin rotation (μSR), nitrogen-vacancy (NV) magnetometry, and nanoscale arrays of superconducting quantum interference devices (nanoSQUIDs). By utilizing these techniques, it should be possible to experimentally constrain parameters, such as the monopole density and hop rate as a function of temperature.

Model. In order to make quantitative predictions we employ the full dipolar spin ice Hamiltonian,

$$H = -J \sum_{\langle (i,a),(j,b)\rangle} \mathbf{S}_i^a \cdot \mathbf{S}_j^b + Dr_{\mathrm{nn}}^3 \sum_{\substack{i>j \\ a,b}} \frac{\mathbf{S}_i^a \cdot \mathbf{S}_j^b}{\left|\mathbf{R}_{ij}^{ab}\right|^3} - \frac{3\left(\mathbf{S}_i^a \cdot \mathbf{R}_{ij}^{ab}\right)\left(\mathbf{S}_j^b \cdot \mathbf{R}_{ij}^{ab}\right)}{\left|\mathbf{R}_{ij}^{ab}\right|^5} \quad (1)$$

for spin vectors $\mathbf{S}_i^a = \sigma_i^a \hat{\mathbf{z}}^a$, where $\sigma_i^a = \pm 1$ and $\hat{\mathbf{z}}^a$ is the local Ising axis at the tetrahedral sublattice site $\mathbf{r}^a$ for fcc lattice site

*franziska.kirschner@physics.ox.ac.uk
†Present address: Rudolf Peierls Centre for Theoretical Physics, University of Oxford, Oxford OX1 3NP, United Kingdom.
‡stephen.blundell@physics.ox.ac.uk

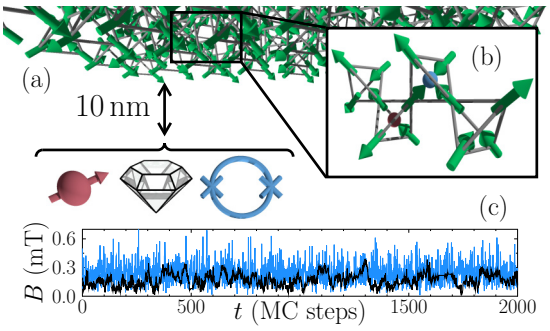

FIG. 1. (a) A schematic of the experimental arrangement for the techniques mentioned in this Rapid Communication with a muon (left), NV in diamond (center), and nanoSQUID (right) acting as ultrasensitive magnetic probes 10 nm from the spin ice. (b) Four adjacent tetrahedra of Dy^{3+} spins, showing the creation of a monopole-antimonopole pair. (c) The field fluctuations 10 nm from the surface in the dipolar spin ice model (DSIM) at 4 K (blue) and 1 K (black).

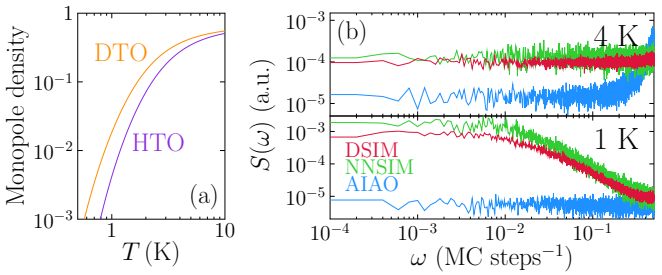

FIG. 2. (a) Evolution of the monopole density in DTO and HTO calculated using Debye-Hückel theory. (b) Frequency dependence of noise spectra $S(\omega)$ for DSIM, NNSIM, and AIAO (see the main text for descriptions of the models) at 4 and 1 K.

$\mathbf{R}_i$. The vector connecting two spins $\mathbf{S}_i^a$ and $\mathbf{S}_j^b$ is thus given by $\mathbf{R}_{ij}^{ab} = \mathbf{R}_{ij} + \mathbf{r}^{ab}$. The exchange energy is $J \approx -3.72$ K for DTO and ≈ -1.56 K for HTO [14,15]. The dipolar energy is $D \approx 1.41$ K for both DTO and HTO [14,15]. The first term in this Hamiltonian corresponds to nearest-neighbor exchange interactions with a nearest-neighbor exchange coupling of $J_{\rm nn} = J/3$ (as the relative orientations of nearest-neighbor $\langle 111 \rangle$ axes give $\hat{\mathbf{z}}^a \cdot \hat{\mathbf{z}}^b = -1/3$). The second term corresponds to long-range dipolar interactions. Although spin ices have been predicted to undergo a first-order phase transition to long-range order below $\sim$0.2 K [16], the equilibration time rises dramatically on cooling and such order has not yet been experimentally detected [13,17,18].

Simulations were carried out on $4 \times 4 \times 4$ unit cells of spin ice using standard Monte Carlo (MC) procedures [19], consisting of 10^4 cooling steps and 5×10^3 steps to measure the stray magnetic fields of the system at temperatures between 4.5 and 0.5 K. Periodic boundary conditions were used in the $\hat{\mathbf{x}}$ and $\hat{\mathbf{y}}$ directions. The probe point for the stray fields is placed 10 nm from the sample in $\hat{\mathbf{z}}$ and the time dependence of the magnetic-field $B(t)$ is calculated by summing the dipolar field produced by all the spins in the film [a schematic of this experimental arrangement is shown in Fig. 1(a)]. MC simulations are often used determine thermal averages. Here their use is restricted to creating a sample spin configuration at a given temperature T then to modeling the spin flip dynamics (and therefore the monopole motion). This approximation has previously been suggested by experimental results [20].

Three different spin arrangements were studied in order to isolate the characteristics of $S(\omega)$ arising from the individual contributions to the Hamiltonian in Eq. (1). This leads us to define three distinct models. (i) The DSIM uses the J and D parameters of DTO. (ii) The nearest-neighbor spin ice model (NNSIM) has no long-range interactions ($D = 0$) but retains the topological constraint from Dirac strings connecting monopoles to antimonopoles. J is chosen so that the monopole density is as for the first case, and $J > 0$ ensures that the two-in-two-out ground state is favored. (3) The all-in-all-out model (AIAO) has $D = 0$ and $J < 0$. The ground state consists of tetrahedra with either four-in or four-out spin configurations. Thermal spin flips in this case are not monopolelike excitations thus providing a control case.

Results. In Fig. 1(c) we show the DSIM prediction for the magnetic field measured at 4 and 1 K. At 4 K most tetrahedra are not in the two-in-two-out state, and a rapidly fluctuating signal is observed. At 1 K the system is close to the ground state with a density of monopoles per tetrahedron of $\approx$0.03 as predicted by Debye-Hückel theory [21]. The monopole density, calculated analytically using the methods described in Ref. [21], is slightly lower in HTO, shown in Fig. 2(a). At this density, most tetrahedra obey the ice rules, but there are sufficiently many monopoles that some may hop across the sample without annihilating, resulting in telegraph noise. By comparison, the AIAO features no qualitative distinction between its high- and low-temperature regimes. The amplitude of the field fluctuations are of order 0.1 mT, well within the experimentally measurable range of the aforementioned techniques.

The time scales in Fig. 1(c) are in units of MC steps, the shortest possible time scale on which a spin flip may occur in the model. There has been considerable debate surrounding the time scale on which spins flip in the physical systems at low temperatures with ac susceptibility measurements suggesting a scale of $\sim$1 ms [22–26] and μSR measurements detecting spin dynamics on a scale of ~ 1 μs [27]. It is possible that this is dependent on the relevant experimental time window (10^0–10^{-4} s for ac susceptibility and 10^{-5}–10^{-11} s for μSR). By performing the nanoscale magnetometry measurements and comparing to the MC time step, the hop rate can be deduced.

In addition to directly probing field fluctuations, complementary information is gained by measuring the noise spectral density $S(\omega)$, given as the Fourier transform of the autocorrelation function $A(\tau) = \int B(t)B(t+\tau)dt$ (see the Supplemental Material [28]). In particular, the latter provides an ability to tune the frequency filter in order to isolate certain dynamical time scales and to compare the amplitude of noise at these time scales. As shown in Fig. 2(b), there is little low-frequency structure in $S(\omega)$ at 4 K, corresponding to very little correlation between the field measurements at different times. Fluctuations are predominantly at the Nyqvist frequency [$\omega_{\rm Ny} = (2 \times \text{MC time step})^{-1}$]. The lack of structure is evident in both DSIM and NNSIM and shows that it would be difficult to discern monopole dynamics within

the temperature range of ^{4}He cryostats. For AIAO, a peak forms at ω_{Ny} as a result of rapid thermal fluctuations. The power spectrum at 1 K, however, shows a clear difference among the DSIM, the NNSIM, and the AIAO cases. The low-frequency structure seen in Fig. 1(c) is manifest in $S(\omega)$. It should be noted that the frequency at which this structure occurs is on the order of $\approx 10^{-2}$ MC steps^{-1}. The DSIM and NNSIM systems both display low-frequency plateaus and a high-frequency power law, which is absent in AIAO. This is a clear indication that the long-range forces play a relatively small role in the monopole dynamics and instead contribute more to the lowering of the overall stray field as evidenced in a smaller area under the $S(\omega)$ curve. This is consistent with other theoretical studies, which suggest that samples are largely dominated by single monopoles as opposed to closely bound pairs [21]. In AIAO, the field fluctuations are smaller and contain no structure on longer time scales, which is expected as it is always energetically favorable for spin flips to undo shortly after creation. We can make quantitative predictions of the functional form of $S(\omega)$ by fitting power laws [$S(\omega) = a\omega^b$] to the low- and high-ω regimes (see also the Supplemental Material [28] for power-law fits of a simpler toy model). DSIM, NNSIM, and AIAO all display low-ω plateaus with $|b| \sim 10^{-2}$. However, in the high-ω regime there are pronounced differences among the three systems. For AIAO, $b > 0$ at both low and high temperatures [$b_{1\,\mathrm{K}}^{\mathrm{AIAO}} = 0.14(5)$, $b_{4\,\mathrm{K}}^{\mathrm{AIAO}} = 4.94(14)$], indicative of a system dominated by thermal spin flips. Both DSIM and NNSIM have $b < 0$ at low temperatures [$b_{1\,\mathrm{K}}^{\mathrm{DSIM}} = -1.29(1)$, $b_{1\,\mathrm{K}}^{\mathrm{NNSIM}} = -1.56(3)$], which increases at high temperatures [$b_{4\,\mathrm{K}}^{\mathrm{DSIM}} = -0.09(2)$, $b_{4\,\mathrm{K}}^{\mathrm{NNSIM}} = -0.08(4)$] as thermal spin flips take over and monopole dynamics are no longer observable.

Experimental techniques. We now consider a number of different nanoscale magnetometry platforms which are promising candidates for detecting monopole behavior in spin ice materials. In addition to providing an analysis of the various regimes of operation, we highlight the complementarity of these measurements. The first experimental technique μSR is usually a bulk probe, but a low-energy variant [29] in which the energy of the muon beam can be continuously varied from 0.5 to 30 keV provides an extension of the technique which allows depth-dependent studies of thin films and multilayered structures in the range from ∼1 to ∼200 nm. This allows for experiments involving proximal magnetometry [30] in which the field close to an ultrathin magnetic layer can be probed. μSR probes fields fluctuating on a time-scale $\sim 10^{-11}$–10^{-5} s. In the cases of zero-field μSR (in which the polarization of the muons is measured in the absence of any external magnetic fields) or longitudinal-field μSR (in which an external field B_{L} is applied along the muon polarization direction), the relaxation rate λ of the muon polarization spectrum can be related to the autocorrelation function of the components of $\mathbf{B}^{\perp}(t)$, the local field transverse to the muon, using $\lambda = \frac{\gamma_\mu^2}{2}\int_0^\infty \langle \mathbf{B}^{\perp}(t)\cdot\mathbf{B}^{\perp}(0)\rangle e^{i\gamma_\mu B_{\mathrm{L}} t}dt$, where γ_μ is the gyromagnetic ratio of the muon. The relaxation rate λ is then proportional to the power spectrum at $\omega = \gamma_\mu B_{\mathrm{L}}$ and so in zero-field measures the zero-frequency part of the power spectrum. Inside spin ice the field at the muon site is very large ∼1 T, but outside the sample the field is dominated by a long-range stray field [27,31]. Our interest here is in the nanoscale field close to the surface at low monopole concentration. We note that the related technique of β-NMR in which low-energy ion implantation of hyperpolarized radioactive magnetic resonance probes are employed instead of muons can also be used in this context [32]. A potential disadvantage of these techniques is that the stopping profile of slow muons or other polarized probes is not sharp so that implantation occurs at a range of depths.

The second method we consider is the use of single spin magnetometery based upon NV point defects in diamond [33,34]. Each NV center constitutes an $S = 1$ electronic spin orientated along one of the four diamond carbon-carbon bond directions. In addition to coherent manipulations via resonant microwave pulses, the NV center's spin state can be optically initialized and detected [35–37]. We envision two possible setups for NV-based monopole magnetometry. The first is a scanning NV magnetometer, consisting of a diamond nanopillar attached to an atomic force microscopy tip [38]. The second entails the placement of the spin ice material in direct proximity to a bulk diamond surface containing a shallow layer of NV centers ∼5–10-nm deep. To detect the characteristic signatures of individual magnetic monopoles, the NV can be utilized in two operational modes: (1) direct measurement of the stray magnetic field from a monopole and (2) spectroscopy of the ac magnetic noise generated by the dynamics and fluctuations of a dilute monopole density.

In the case of dc magnetometry, one would observe Zeeman shifts in the NV resonance frequency (e.g., between the $|m_s = 0\rangle$ and the $|m_s = -1\rangle$ spin states) in real time in order to measure the stray field of a monopole as it passes through the sensing volume of a single shallow NV center (Fig. 1). This can be achieved using either Ramsey spectroscopy or continuous-wave optically detected magnetic resonance spectroscopy. The field sensitivity of this approach is limited by T_2^*, the NV dephasing time, leading to a sensitivity of $\sim 5\ \mu\mathrm{T}/\sqrt{\mathrm{Hz}}$ [39]. Assuming an integration time of ∼250 μs this enables a field sensitivity of ∼0.3 mT and a corresponding dc sensing volume of ∼10 nm surrounding the NV center. This sensitivity is sufficient to detect the real-time dynamics of individual monopoles (see Fig. 1).

For ac magnetometry, we are interested in the individual Fourier components of the time-varying magnetic field generated by the dynamics of a low density of magnetic monopoles. To generate such a frequency filter, the NV center is manipulated using a series of periodic microwave pulses separated by a free-evolution time τ. This modulation creates a narrow bandpass frequency filter at $1/\tau$; by varying the free-evolution time, one can map out the noise spectral density associated with magnetic fluctuations. Compared to the dc case, the key advantage of this approach is that the field sensitivity is no longer limited by T_2^*, but rather by T_2, the intrinsic spin decoherence time of the NV center. For shallow-implanted NVs, this yields a field sensitivity of $\sim 50\ \mathrm{nT}/\sqrt{\mathrm{Hz}}$ [39]. Assuming an integration time of ≈250 μs this enables a field sensitivity of ≈3 μT, which is well within the desired sensitivity.

The third experimental method employs nanoSQUIDs. The SQUID is an extremely sensitive detector of magnetic flux, and decreasing its size leads to a highly versatile sensor of local

magnetic fields [40,41] with a spin sensitivity that has reached below a single Bohr magneton [42].

The experimental techniques considered in this Rapid Communication have different advantages and drawbacks. The nanoSQUID technique, despite excellent sensitivity and the ability to work at the required temperature regime, may suffer from a large spatial averaging of fields across the area of the sensor ($\sim 10^5$ nm^2). This is much larger than that for the polarized probes and NV centers for which the active sensor is essentially pointlike. Low-energy muons, although point probes, can only be implanted over a range of depths. Thus a suitable overlayer can be deposited on the surface of spin ice and muons implanted into it, but the observed signal will average over a spread of distances between the spin ice surface and the probe, although the mean distance can be varied by varying the implantation energy. NV centers may be much better in this regard, although measurements need to be obtained with an applied magnetic field, which is not the case for μSR.

At the time of writing, both μSR and NV-magnetometry experiments are limited to temperatures above 4.2 K by the use of ^{4}He cryostats. When such experiments are able to reach temperatures of ≈ 1.5 K, there are clearly discernible qualitative signatures of two key characteristics of magnetic monopoles: their Coulomb interaction and topological constraints deriving from Dirac strings. Unconstrained thermal spin flips feature a Debye-type noise spectral density, matching that of Brownian motion, with a low-frequency plateau followed by a turnover to inverse-square flicker noise at characteristic time-scale τ. Coulomb interactions between Brownian particles decrease the tim-scale τ through recombination of particle/antiparticle pairs. In general, one expects a range of time scales to be important in $S(\omega)$ originating from a slowing of dynamics heading out of equilibrium at the lowest temperatures. The nanoscale probes proposed in this Rapid Communication can cover a wide range of time-scales from 10^0 to 10^{-4} s (NV magnetometers) through 10^{-5} to 10^{-11} s (μSR) in order to probe the relevant dynamics and to understand the scaling between experimental time scales and those used in MC simulations, both of which can be tuned by temperature.

The effect of the sample surface is an important consideration due to the possible presence of surface magnetic charges [43,44]; this effect can be studied by measuring samples cleaved perpendicular to different crystallographic directions (see the Supplemental Material [28]).

Two further modes of operation which can be used in the identification and characterization of monopoles with these probes are as follows. We note the possibility of making two-point correlation measurements using two probes in NV magnetometry. Such measurements could be used to time the motion of single monopoles, helping constrain system parameters, such as the magnetic charge when used in combination with applied B fields. A further possibility is to use one magnetized tip and one measurement tip to probe the response to local perturbations.

To summarize, we have presented a road map for future experiments of monopole behavior using nanoscale magnetic probes of the noise spectrum of the dipolar field measured very close to the surface of spin ice. The techniques have varying advantages and disadvantages and need to be extended to the 1-K regime where the monopole density is sufficiently low that observation of individual magnetic monopoles is possible. Such an observation would open up an era of direct measurement of monopole transport in these topologically constrained systems and provide new insight into the classical $U(1)$ spin liquid.

Acknowledgments. The authors would like to thank M. J. P. Gingras and D. Santamore for helpful discussions. We thank EPSRC (U.K.) for funding support under grant EP/N023803/1. F.K.K.K. thanks Lincoln College Oxford for a doctoral studentship. F.F. acknowledges support from a Lindemann Trust Fellowship of the English Speaking Union and an Astor Junior Research Fellowship from New College, Oxford. N.Y.Y. was supported by the LDRD Program of LBNL under U.S. DOE Contract No. DE-AC02-05CH11231. A.Y. was supported by the Gordon and Betty Moore Foundation's Emergent Phenomena in Quantum Systems (EPiQS) Initiative through Grant No. GBMF4531. A.Y. was also partly supported by Army Research Office Grant No. W911NF-17-1-0023.

[1] K. A. Milton, Rep. Prog. Phys. **69**, 1637 (2006).
[2] M. J. Harris, S. T. Bramwell, D. F. McMorrow, T. Zeiske, and K. W. Godfrey, Phys. Rev. Lett. **79**, 2554 (1997).
[3] C. Castelnovo, R. Moessner, and S. L. Sondhi, Nature (London) **451**, 42 (2008).
[4] I. A. Ryzhkin, JETP **101**, 481 (2005).
[5] D. J. P. Morris, D. A. Tennant, S. A. Grigera, B. Klemke, C. Castelnovo, R. Moessner, C. Czternasty, M. Meissner, K. C. Rule, J.-U. Hoffmann, K. Kiefer, S. Gerischer, D. Slobinsky, and R. S. Perry, Science **326**, 411 (2009).
[6] L. Pauling, J. Am. Chem. Soc. **57**, 2680 (1935).
[7] D. A. Huse, W. Krauth, R. Moessner, and S. L. Sondhi, Phys. Rev. Lett. **91**, 167004 (2003).
[8] S. V. Isakov, K. Gregor, R. Moessner, and S. L. Sondhi, Phys. Rev. Lett. **93**, 167204 (2004).
[9] C. L. Henley, Phys. Rev. B **71**, 014424 (2005).
[10] T. Fennell, P. P. Deen, A. R. Wildes, K. Schmalzl, D. Prabhakaran, A. T. Boothroyd, R. J. Aldus, D. F. McMorrow, and S. T. Bramwell, Science **326**, 415 (2009).
[11] C. L. Henley, Annu. Rev. Condens. Matter Phys. **1**, 179 (2010).
[12] M. Hermele, M. P. A. Fisher, and L. Balents, Phys. Rev. B **69**, 064404 (2004).
[13] D. Pomaranski, L. R. Yaraskavitch, S. Meng, K. A. Ross, H. M. L. Noad, H. A. Dabkowska, B. D. Gaulin, and J. B. Kycia, Nat. Phys. **9**, 353 (2013).
[14] B. C. den Hertog and M. J. P. Gingras, Phys. Rev. Lett. **84**, 3430 (2000).
[15] S. T. Bramwell, M. J. Harris, B. C. den Hertog, M. J. P. Gingras, J. S. Gardner, D. F. McMorrow, A. R. Wildes, A. Cornelius, J. D. M. Champion, R. G. Melko, and T. Fennell, Phys. Rev. Lett. **87**, 047205 (2001).

[16] R. G. Melko, B. C. den Hertog, and M. J. P. Gingras, Phys. Rev. Lett. **87**, 067203 (2001).
[17] K. Matsuhira, C. Paulsen, E. Lhotel, C. Sekine, Z. Hiroi, and S. Takagi, J. Phys. Soc. Jpn. **80**, 123711 (2011).
[18] P. Henelius, T. Lin, M. Enjalran, Z. Hao, J. G. Rau, J. Altosaar, F. Flicker, T. Yavors'kii, and M. J. P. Gingras, Phys. Rev. B **93**, 024402 (2016).
[19] N. Metropolis, A. W. Rosenbluth, M. N. Rosenbluth, A. H. Teller, and E. Teller, J. Chem. Phys. **21**, 1087 (1953).
[20] L. Bovo, J. A. Bloxsom, D. Prabhakaran, G. Aeppli, and S. T. Bramwell, Nat. Commun. **4**, 1535 (2013).
[21] C. Castelnovo, R. Moessner, and S. L. Sondhi, Phys. Rev. B **84**, 144435 (2011).
[22] J. Snyder, B. G. Ueland, J. S. Slusky, H. Karunadasa, R. J. Cava, and P. Schiffer, Phys. Rev. B **69**, 064414 (2004).
[23] L. D. C. Jaubert and P. C. W. Holdsworth, Nat. Phys. **5**, 258 (2009).
[24] J. A. Quilliam, L. R. Yaraskavitch, H. A. Dabkowska, B. D. Gaulin, and J. B. Kycia, Phys. Rev. B **83**, 094424 (2011).
[25] V. Kaiser, S. T. Bramwell, P. C. W. Holdsworth, and R. Moessner, Phys. Rev. Lett. **115**, 037201 (2015).
[26] B. Tomasello, C. Castelnovo, R. Moessner, and J. Quintanilla, Phys. Rev. B **92**, 155120 (2015).
[27] J. Lago, S. J. Blundell, and C. Baines, J. Phys.: Condens. Matter **19**, 326210 (2007).
[28] See Supplemental Material at http://link.aps.org/supplemental/10.1103/PhysRevB.97.140402 for phenomenological forms of the noise spectrum, additional simulations, and a discussion of surface effects.
[29] E. Morenzoni, T. Prokscha, A. Suter, H. Luetkens, and R. Khasanov, J. Phys.: Condens. Matter **16**, S4583 (2004).
[30] Z. Salman and S. Blundell, Phys. Procedia **30**, 168 (2012).
[31] S. J. Blundell, Phys. Rev. Lett. **108**, 147601 (2012).
[32] M. Xu, M. Hossain, H. Saadaoui, T. Parolin, K. Chow, T. Keeler, R. Kiefl, G. Morris, Z. Salman, Q. Song, D. Wang, and W. MacFarlane, J. Magn. Reson. **191**, 47 (2008).
[33] L. Rondin, J. P. Tetienne, T. Hingant, J. F. Roch, P. Maletinsky, and V. Jacques, Rep. Prog. Phys. **77**, 056503 (2013).
[34] I. Lovchinsky, A. O. Sushkov, E. Urbach, N. P. de Leon, S. Choi, K. De Greve, R. Evans, R. Gertner, E. Bersin, C. Müller, L. McGuinness, F. Jelezko, R. L. Walsworth, H. Park, and M. D. Lukin, Science **351**, 836 (2016).
[35] L. Childress, M. V. Gurudev Dutt, J. M. Taylor, A. S. Zibrov, F. Jelezko, J. Wrachtrup, P. R. Hemmer, and M. D. Lukin, Science **314**, 281 (2006).
[36] J. R. Maze, P. L. Stanwix, J. S. Hodges, S. Hong, J. M. Taylor, P. Cappellaro, L. Jiang, M. V. G. Dutt, E. Togan, A. S. Zibrov, A. Yacoby, R. L. Walsworth, and M. D. Lukin, Nature (London) **455**, 644 (2008).
[37] F. Shi, Q. Zhang, P. Wang, H. Sun, J. Wang, X. Rong, M. Chen, C. Ju, F. Reinhard, H. Chen, J. Wrachtrup, J. Wang, and J. Du, Science **347**, 1135 (2015).
[38] M. S. Grinolds, S. Hong, S. P. Maletinsky, L. Luan, M. D. Lukin, R. L. Walsworth, and A. Yacoby, Nat. Phys. **9**, 215 (2013).
[39] P. Maletinsky, S. Hong, M. S. Grinolds, B. Hausmann, M. D. Lukin, R. L. Walsworth, M. Loncar, and A. Yacoby, Nat. Nanotechnol. **7**, 320 (2012).
[40] W. Wernsdorfer, Supercond. Sci. Technol. **22**, 064013 (2009).
[41] C. Granata and A. Vettoliere, Phys. Rep. **614**, 1 (2016).
[42] D. Vasyukov, Y. Anahory, L. Embon, D. Halbertal, J. Cuppens, L. Neeman, A. Finkler, Y. Segev, Y. Myasoedov, M. L. Rappaport, M. E. Huber, and E. Zeldov, Nat. Nanotechnol. **8**, 639 (2013).
[43] L. D. C. Jaubert, T. Lin, T. S. Opel, P. C. W. Holdsworth, and M. J. P. Gingras, Phys. Rev. Lett. **118**, 207206 (2017).
[44] É. Lantagne-Hurtubise, J. G. Rau, and M. J. P. Gingras, arXiv:1709.00012.